

On the Subspace of Image Gradient Orientations

Georgios Tzimiropoulos and Stefanos Zafeiriou

Imperial College London

Abstract

We introduce the notion of Principal Component Analysis (PCA) of image gradient orientations. As image data is typically noisy, but noise is substantially different from Gaussian, traditional PCA of pixel intensities very often fails to estimate reliably the low-dimensional subspace of a given data population. We show that replacing intensities with gradient orientations and the ℓ_2 norm with a cosine-based distance measure offers, to some extent, a remedy to this problem. Our scheme requires the eigen-decomposition of a covariance matrix and is as computationally efficient as standard ℓ_2 PCA. We demonstrate some of its favorable properties on robust subspace estimation.

Index Terms

Principal Component Analysis, gradient orientations, cosine kernel

NOTATION

$\mathcal{S}, \{.\}$	set
\mathfrak{R}	set of reals
\mathcal{C}	set of complex numbers
x	scalar
\mathbf{x}	column vector
\mathbf{X}	matrix
$\mathbf{I}_{m \times m}$	$m \times m$ identity matrix
$\mathbf{a}(k)$	k -th element of vector \mathbf{a}
$N(\mathcal{S})$	cardinality set \mathcal{S}
$\ \cdot\ $	ℓ_2 norm
$\ \cdot\ _F$	Frobenius norm
\mathbf{Z}^H	conjugate transpose of \mathbf{Z}
$U[a, b]$	uniform distribution in $[a, b]$
$\mathbb{E}[\cdot]$	mean value operator
$x \sim U[a, b]$	x follows $U[a, b]$

I. INTRODUCTION

Provision for mechanisms capable of handling gross errors caused by possible arbitrarily large model deviations is a typical prerequisite in computer vision. Such deviations are not unusual in real-world applications where data contain artifacts due to occlusions, illumination changes, shadows, reflections or the appearance of new parts/objects. In most cases, such phenomena cannot be described by a mathematically well-defined generative model and are usually referred as outliers in learning and parameter estimation.

In this paper, we propose a new avenue for Principal Component Analysis (PCA), perhaps the most classical tool for dimensionality reduction and feature extraction in pattern recognition. Standard PCA estimates the k -rank linear subspace of the given data population, which is optimal in a least-squares sense. Unfortunately ℓ_2 norm enjoys optimality properties only when noise is i.i.d. Gaussian; for data corrupted by outliers, the estimated subspace can be arbitrarily biased.

Robust formulations to PCA, such as robust covariance matrix estimators [1], [2], are computationally prohibitive for high dimensional data such as images. Robust approaches, well-suited for computer vision applications, include ℓ_1 [3], [4], robust energy function [5] and weighted combination of nuclear norm and ℓ_1 minimization [6], [7]. ℓ_1 -based approaches can be computationally efficient, however the gain in robustness is not always significant. The M-Estimation framework of [5] is robust but suitable only for relatively low dimensional data or off-line processing. Under weak assumptions [7], the convex optimization formulation of [6], [7] perfectly recovers the low dimensional subspace of a data population corrupted by sparse arbitrarily large errors; nevertheless efficient reformulations of standard PCA can be orders of magnitude faster.

In this paper we look at robust PCA from a completely different perspective. Our scheme *does not* operate on pixel intensities. In particular, we replace pixel intensities with gradient orientations. We define a notion of pixel-wise image dissimilarity by looking at the distribution of gradient orientation differences; intuitively this must be approximately uniform in $[0, 2\pi)$. We then assume that local orientation mismatches caused by outliers can be also well-described by a uniform distribution which, under some mild assumptions, is canceled out when we apply the cosine kernel. This last observation has been noticed in recently proposed schemes for image registration [8]. Following this line of research, we show that a cosine-based distance measure has a functional form which enables us to define an explicit mapping from the space of gradient orientations into a high-dimensional complex sphere where essentially linear complex PCA is performed. The mapping is one-to-one and therefore PCA-based reconstruction in the original input space is direct and requires no further optimization. Similarly to standard PCA, the basic computational module of our scheme requires the eigen-decomposition of a covariance matrix, while high dimensional data can be efficiently analyzed following the strategy suggested in Turk and Pentland's Eigenfaces [9].

II. ℓ_2 -BASED PCA OF PIXEL INTENSITIES

Let us denote by $\mathbf{x}_i \in \mathfrak{R}^p$ the p -dimensional vector obtained by writing image $\mathbf{I}_i \in \mathfrak{R}^{m_1 \times m_2}$ in lexicographic ordering. We assume that we are given a population of n samples $\mathbf{X} = [\mathbf{x}_1 | \cdots | \mathbf{x}_n] \in \mathfrak{R}^{p \times n}$. Without loss of generality, we assume zero-mean data. PCA finds a set

of $k < n$ orthonormal bases $\mathbf{B}_k = [\mathbf{b}_1 | \dots | \mathbf{b}_k] \in \mathfrak{R}^{p \times k}$ by minimizing the error function

$$\epsilon(\mathbf{B}_k) = \|\mathbf{X} - \mathbf{B}_k \mathbf{B}_k^T \mathbf{X}\|_F^2. \quad (\text{II.1})$$

The solution is given by the eigenvectors corresponding to the k largest eigenvalues obtained from the eigen-decomposition of the covariance matrix $\mathbf{X}\mathbf{X}^T$. Finally, the reconstruction of \mathbf{X} from the subspace spanned by the columns of \mathbf{B}_k is given by $\tilde{\mathbf{X}} = \mathbf{B}_k \mathbf{C}_k$, where $\mathbf{C}_k = \mathbf{B}_k^T \mathbf{X}$ is the matrix which gathers the set of projection coefficients.

For high dimensional data and Small Sample Size (SSS) problems (i.e. $n \ll p$), an efficient implementation of PCA in $O(n^3)$ (instead of $O(p^3)$) was proposed in [9]. Rather than computing the eigen-analysis of $\mathbf{X}\mathbf{X}^T$, we compute the eigen-analysis of $\mathbf{X}^T \mathbf{X}$ and make use of the following theorem

Theorem I

Define matrices \mathbf{A} and \mathbf{B} such that $\mathbf{A} = \mathbf{\Gamma}\mathbf{\Gamma}^H$ and $\mathbf{B} = \mathbf{\Gamma}^H \mathbf{\Gamma}$ with $\mathbf{\Gamma} \in \mathcal{C}^{m \times r}$. Let \mathbf{U}_A and \mathbf{U}_B be the eigenvectors corresponding to the non-zero eigenvalues Λ_A and Λ_B of \mathbf{A} and \mathbf{B} , respectively. Then, $\Lambda_A = \Lambda_B$ and $\mathbf{U}_A = \mathbf{\Gamma}\mathbf{U}_B\Lambda_A^{-\frac{1}{2}}$.

III. RANDOM NUMBER GENERATION FROM GRADIENT ORIENTATION DIFFERENCES

We formalize an observation for the distribution of gradient orientation differences which does not appear to be well-known in the scientific community ¹. Consider a set of images $\{\mathbf{J}_i\}$. At each pixel location, we estimate the image gradients and the corresponding gradient orientation ². We denote by $\{\Phi_i\}$, $\Phi_i \in [0, 2\pi)^{m_1 \times m_2}$ the set of orientation images and compute the orientation difference image

$$\Delta\Phi_{ij} = \Phi_i - \Phi_j. \quad (\text{III.1})$$

We denote by ϕ_i and $\Delta\phi_{ij} \triangleq \phi_i - \phi_j$ the p -dimensional vectors obtained by writing Φ_i and $\Delta\Phi_{ij}$ in lexicographic ordering and $\mathcal{P} = \{1, \dots, p\}$ the set of indices corresponding to the image support. We introduce the following definition.

Definition Images \mathbf{J}_i and \mathbf{J}_j are pixel-wise dissimilar if $\forall k \in \mathcal{P}$, $\Delta\phi_{ij}(k) \sim U[0, 2\pi)$.

¹This observation has been somewhat noticed in [10] with no further comments on its implications.

²More specifically, we compute $\Phi_i = \arctan G_{i,y}/G_{i,x}$, where $G_{i,x} = h_x \star I_i$, $G_{i,y} = h_y \star I_i$ and h_x, h_y are filters used to approximate the ideal differentiation operator along the image horizontal and vertical direction respectively. Possible choices for h_x, h_y include central difference estimators of various orders and discrete approximations to the first derivative of the Gaussian.

Not surprisingly, nature is replete with images exemplifying Definition 1. This, in turn, makes it possible to set up a naive image-based random generator. To confirm this, we used more than 70,000 pairs of image patches of resolution 200×200 randomly extracted from natural images [11]. For each pair, we computed $\Delta\phi_{ij}$ and formulated the following null hypothesis

- $H_0: \forall k \in \mathcal{P} \Delta\phi_{ij}(k) \sim U[0, 2\pi)$.

which was tested using the Kolmogorov-Smirnov test [12]. For a significance level equal to 0.01, the null hypothesis was accepted for 94.05% of the image pairs with mean p -value equal to 0.2848. In a similar setting, we tested Matlab’s random generator. The null hypothesis was accepted for 99.48% of the cases with mean p -value equal to 0.501. Fig. 1 (a)-(b) show a typical pair of image patches considered in our experiment. Fig. 1 (c) and (d) plot the histograms of the gradient orientation differences and 40,000 samples drawn from Matlab’s random number generator respectively.

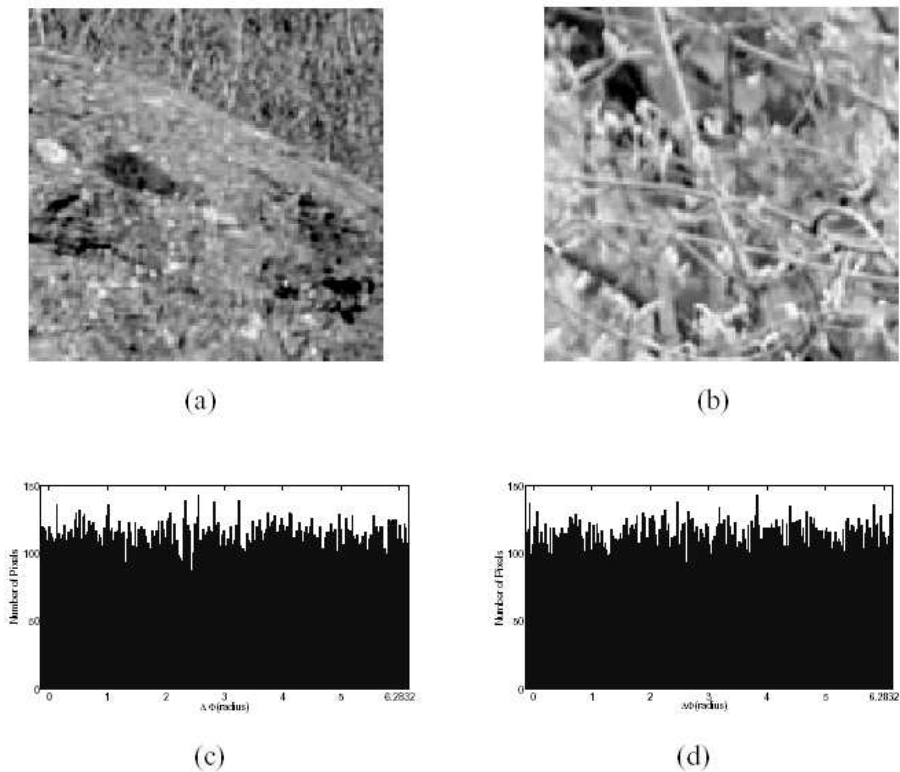


Fig. 1. (a)-(b) An image pair used in our experiment, (c) Image-based random number generator: histogram of 40,000 gradient orientation differences and (d) Histogram of 40,000 samples drawn from Matlab’s random number generator.

IV. PCA OF GRADIENT ORIENTATIONS

A. Cosine-based correlation of gradient orientations

Given the set of our images $\{\mathbf{I}_i\}$, we compute the corresponding set of orientation images $\{\Phi_i\}$ and measure image correlation using the cosine kernel

$$s(\phi_i, \phi_j) \triangleq \sum_{k \in \mathcal{P}} \cos[\Delta\phi_{ij}(k)] = cN(\mathcal{P}) \quad (\text{IV.1})$$

where $c \in [-1, 1]$. Notice that for highly spatially correlated images $\Delta\phi_{ij}(k) \approx 0$ and $c \rightarrow 1$.

Assume that there exists a subset $\mathcal{P}_2 \subset \mathcal{P}$ corresponding to the set of pixels corrupted by outliers. For $\mathcal{P}_1 = \mathcal{P} - \mathcal{P}_2$, we have

$$s_1(\phi_i, \phi_j) = \sum_{k \in \mathcal{P}_1} \cos[\Delta\phi_{ij}(k)] = c_1N(\mathcal{P}_1) \quad (\text{IV.2})$$

where $c_1 \in [-1, 1]$.

Not unreasonably, we assume that in \mathcal{P}_2 , the images are pixel-wise dissimilar according to Definition 1. For example, Fig. 2 (a)-(b) show an image pair where \mathcal{P}_2 is the part of the face occluded by the scarf and Fig. 2 (c) plots the distribution of $\Delta\phi$ in \mathcal{P}_2 . Before proceeding for

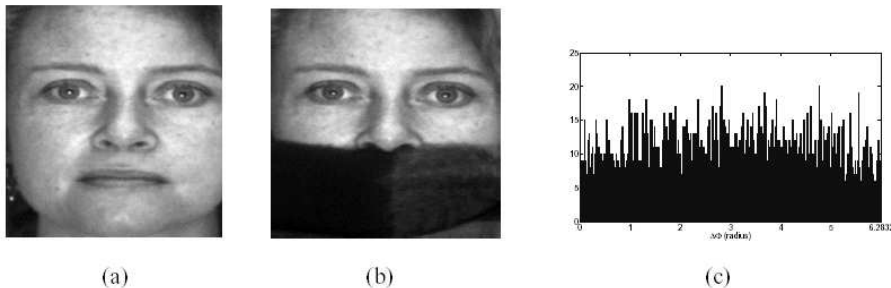


Fig. 2. (a)-(b) An image pair used in our experiments. (c) The distribution of $\Delta\phi$ for the part of face occluded by the scarf.

\mathcal{P}_2 , we need the following theorem [12].

Theorem II

Let $u(\cdot)$ be a random process and $u(t) \sim U[0, 2\pi)$ then:

- $\mathbb{E}[\int_{\mathcal{X}} \cos u(t) dt] = 0$ for any non-empty interval \mathcal{X} of \mathfrak{R} .
- If $u(\cdot)$ is mean ergodic, then $\int_{\mathcal{X}} \cos u(t) dt = 0$.

We also make use of the following approximation

$$\int_{\mathcal{X}} \cos[\Delta\phi_{ij}(t)] dt \approx \sum_{k \in \mathcal{P}} \cos[\Delta\phi_{ij}(k)] \quad (\text{IV.3})$$

where with some abuse of notation, $\Delta\phi_{ij}$ is defined in the continuous domain on the left hand side of (IV.3). Completely analogously, the above theorem and approximation hold for the case of the sine kernel.

Using the above results, for \mathcal{P}_2 , we have

$$s_2(\phi_i, \phi_j) = \sum_{k \in \mathcal{P}_2} \cos[\Delta\phi_{ij}(k)] \simeq 0 \quad (\text{IV.4})$$

It is not difficult to verify that ℓ_2 -based correlation i.e. the inner product between two images will be zero if and only if the images have interchangeably black and white pixels. Our analysis and (IV.4) show that cosine-based correlation of gradient orientations allows for a much broader class of uncorrelated images. Overall, unlike ℓ_2 -based correlation where the contribution of outliers can be arbitrarily large, $s(\cdot)$ measures correlation as $s(\phi_i, \phi_j) = s_1(\phi_i, \phi_j) + s_2(\phi_i, \phi_j) \simeq c_1 N(\mathcal{P}_1)$, i.e. the effect of outliers is approximately canceled out.

B. The principal components of image gradient orientations

To show how (IV.1) can be used as a basis for PCA, we first define the distance

$$d^2(\phi_i, \phi_j) = \sum_{k=1}^p \{1 - \cos[\Delta\phi_{ij}(k)]\} \quad (\text{IV.5})$$

We can write (IV.5) as follows

$$\begin{aligned} d^2(\phi_i, \phi_j) &= \frac{1}{2} \sum_{k=1}^p \{2 - 2 \cos[\phi_i(k) - \phi_j(k)]\} \\ &= \frac{1}{2} \|e^j \phi_i - e^j \phi_j\|^2 \end{aligned} \quad (\text{IV.6})$$

where $e^j \phi_i = [e^j \phi_i^{(1)}, \dots, e^j \phi_i^{(p)}]^T$. The last equality makes the basic computational module of our scheme apparent. We define the mapping from $[0, 2\pi)^p$ onto a subset of complex sphere with radius $\sqrt{N(\mathcal{P})}$

$$\mathbf{z}_i(\phi_i) = e^j \phi_i \quad (\text{IV.7})$$

and apply linear complex PCA to the transformed data \mathbf{z}_i .

Using the results of the previous subsection, we can remark the following

Remark I If $\mathcal{P} = \mathcal{P}_1 \cup \mathcal{P}_2$ with $\Delta\phi_{ij}(k) \sim U[0, 2\pi)$, $\forall k \in \mathcal{P}_2$, then $\text{Re}[\mathbf{z}_i^H \mathbf{z}_j] \simeq c_1 N(\mathcal{P}_1)$

Remark II If $\mathcal{P}_2 = \mathcal{P}$, then $\text{Re}[\mathbf{z}_i^H \mathbf{z}_j] \simeq 0$ and $\text{Im}[\mathbf{z}_i^H \mathbf{z}_j] \simeq 0$.

Further geometric intuition about the mapping \mathbf{z}_i is provided by the chord between vectors \mathbf{z}_i and \mathbf{z}_j

$$\text{crd}(\mathbf{z}_i, \mathbf{z}_j) = \sqrt{(\mathbf{z}_i - \mathbf{z}_j)^H (\mathbf{z}_i - \mathbf{z}_j)} = \sqrt{2d^2(\phi_i, \phi_j)} \quad (\text{IV.8})$$

Using $\text{crd}(\cdot)$, the results of Remark 1 and 2 can be reformulated as $\text{crd}(\mathbf{z}_i, \mathbf{z}_j) \simeq \sqrt{2((1 - c_1)N(\mathcal{P}_1) + N(\mathcal{P}_2))}$ and $\text{crd}(\mathbf{z}_i, \mathbf{z}_j) \simeq \sqrt{2N(\mathcal{P})}$ respectively.

Overall, **Algorithm 1** summarizes the steps of our PCA of gradient orientations.

Algorithm 1. *Estimating the principal subspace*

Inputs: A set of n orientation images Φ_i , $i = 1, \dots, n$ of p pixels and the number k of principal components.

Step 1. Obtain ϕ_i by writing Φ_i in lexicographic ordering.

Step 2. Compute $\mathbf{z}_i = e^{j\phi_i}$, form the matrix of the transformed data $\mathbf{Z} = [\mathbf{z}_1 | \dots | \mathbf{z}_n] \in \mathcal{C}^{p \times n}$ and compute the matrix $\mathbf{T} = \mathbf{Z}^H \mathbf{Z} \in \mathcal{R}^{n \times n}$.

Step 3. Compute the eigen-decomposition of $\mathbf{T} = \mathbf{U}\mathbf{\Lambda}\mathbf{U}^H$ and denote by $\mathbf{U}_k \in \mathcal{C}^{p \times k}$ and $\mathbf{\Lambda}_k \in \mathcal{R}^{k \times k}$ the k -reduced set. Compute the principal subspace from $\mathbf{B}_k = \mathbf{Z}\mathbf{U}_k\mathbf{\Lambda}_k^{-\frac{1}{2}} \in \mathcal{C}^{p \times k}$.

Step 4. Reconstruct using $\tilde{\mathbf{Z}} = \mathbf{B}_k\mathbf{B}_k^H\mathbf{Z}$.

Step 5. Go back to the orientation domain using $\tilde{\Phi} = \angle\tilde{\mathbf{Z}}$.

Let us denote by $\mathcal{Q} = \{1, \dots, n\}$ the set of image indices and \mathcal{Q}_i any subset of \mathcal{Q} . We can conclude the following

Remark III If $\mathcal{Q} = \mathcal{Q}_1 \cup \mathcal{Q}_2$ with $\mathbf{z}_i^H \mathbf{z}_j \simeq 0 \forall i \in \mathcal{Q}_2, \forall j \in \mathcal{Q}$ and $i \neq j$, then, \exists eigenvector \mathbf{b}_l of \mathbf{B}_n such that $\mathbf{b}_l \simeq \frac{1}{N(\mathcal{P})}\mathbf{z}_i$.

A special case of Remark III is the following

Remark IV If $\mathcal{Q} = \mathcal{Q}_2$, then $\frac{1}{N(\mathcal{P})}\mathbf{\Lambda} \simeq \mathbf{I}_{n \times n}$ and $\mathbf{B}_n \simeq \frac{1}{N(\mathcal{P})}\mathbf{Z}$.

To exemplify Remark IV, we computed the eigen-spectrum of 100 natural image patches. In a similar setting, we computed the eigen-spectrum of samples drawn from Matlab's random number generator. Fig. 3 plots the two eigen-spectrums.

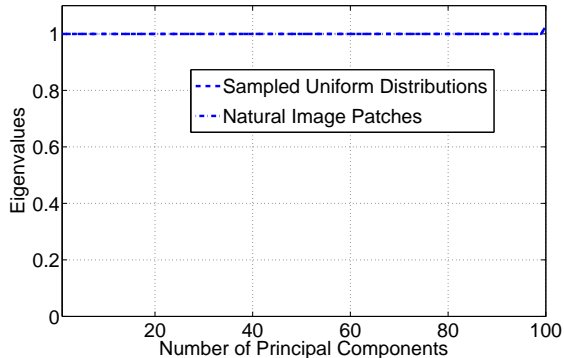


Fig. 3. The eigen-spectrum of natural images and the eigen-spectrum of samples drawn from Matlab’s random number generator.

Finally, notice that our framework also enables the direct embedding of new samples. **Algorithm 2** summarizes the procedure.

Algorithm 2. *Embedding of new samples*

Inputs: An orientation image Θ of p pixels and the principal subspace \mathbf{B}_k of **Algorithm 1**.

Step 1. Obtain θ by writing Θ in lexicographic ordering.

Step 2. Compute $\mathbf{z} = e^{j\theta}$ and reconstruct using $\tilde{\mathbf{z}} = \mathbf{B}_k \mathbf{B}_k^H \mathbf{z}$.

Step 3. Go back to the orientation domain using $\tilde{\theta} = \angle \tilde{\mathbf{z}}$.

V. RESULTS

A. Face reconstruction

The estimation of a low-dimensional subspace from a set of a highly-correlated images is a typical application of PCA [13]. As an example, we considered a set of 50 aligned face images of image resolution 192×168 taken from the Yale B face database [14]. The images capture the face of the same subject under different lighting conditions. This setting usually induces cast shadows as well as other specularities. Face reconstruction from the principal subspace is a natural candidate for removing these artifacts.

We initially considered two versions of this experiment. The first version used the set of original images. In the second version, 20% of the images was artificially occluded by a 70×70 “Baboon” patch placed at random spatial locations. For both experiments, we reconstructed pixel intensities and gradient orientations with ℓ_2 PCA and PCA of gradient orientations respectively using the first 5 principal components.

Fig. 4 and Fig. 5 illustrate the quality of reconstruction for 2 examples of face images considered in our experiments. While PCA-based reconstruction of pixel intensities is visually appealing in the first experiment, Fig. 4 (g)-(h) clearly illustrate that, in the second experiment, the reconstruction suffers from artifacts. In contrary, Fig. 5 (e)-(f) and (g)-(h) show that PCA-based reconstruction of gradient orientations not only reduces the effect of specularities but also reconstructs the gradient orientations corresponding to the “face” component only.

This performance improvement becomes more evident by plotting the principal components for each method and experiment. Fig. 6 shows the 5 dominant Eigenfaces of ℓ_2 PCA. Observe that, in the second experiment, the last two Eigenfaces (Fig. 6 (i) and (j)) contain “Baboon” ghosts which largely affect the quality of reconstruction. In contrary, a simple visual inspection of Fig. 7 reveals that, in the second experiment, the principal subspace of gradient orientations (Fig. 7 (f)-(j)) is artifact-free which in turn makes dis-occlusion in the orientation domain feasible.

Finally, to exemplify Remark 3, we considered a third version of our experiment where 20% of the images were replaced by *the same* 192×168 “Baboon” image. Fig. 8 (a)-(e) and (f)-(j) illustrate the principal subspace of pixel intensities and gradient orientations respectively. Clearly, we may observe that ℓ_2 PCA was unable to handle the extra-class outlier. In contrary, PCA of gradient orientations successfully separated the “face” from the “Baboon” subspace i.e. no eigenvectors were corrupted by the “Baboon” image. Note that the “face” principal subspace is not the same as the one obtained in versions 1 and 2. This is because only 80% of the images in our dataset was used in this experiment.

VI. CONCLUSIONS

We introduced a new concept: PCA of gradient orientations. Our framework is as simple as standard ℓ_2 PCA, yet much more powerful for efficient subspace-based data representation. Central to our analysis is the distribution of gradient orientation differences and the cosine kernel which provide us a consistent way to measure image dissimilarity. We showed how this dissimilarity measure can be naturally used to formulate a robust version of PCA. Extensions of our scheme span a wide range of theoretical topics and applications; from statistical machine learning and clustering to object recognition and tracking.

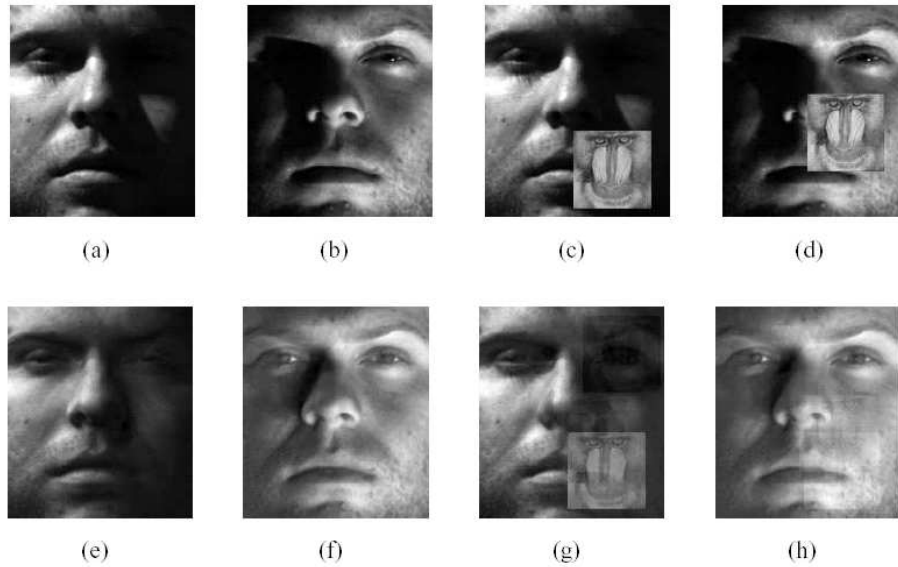


Fig. 4. PCA-based reconstruction of pixel intensities. (a)-(b) Original images used in version 1 of our experiment. (c)-(d) Corrupted images used in version 2 of our experiment. (e)-(f) Reconstruction of (a)-(b) with 5 principal components. (g)-(h) Reconstruction of (c)-(d) with 5 principal components.

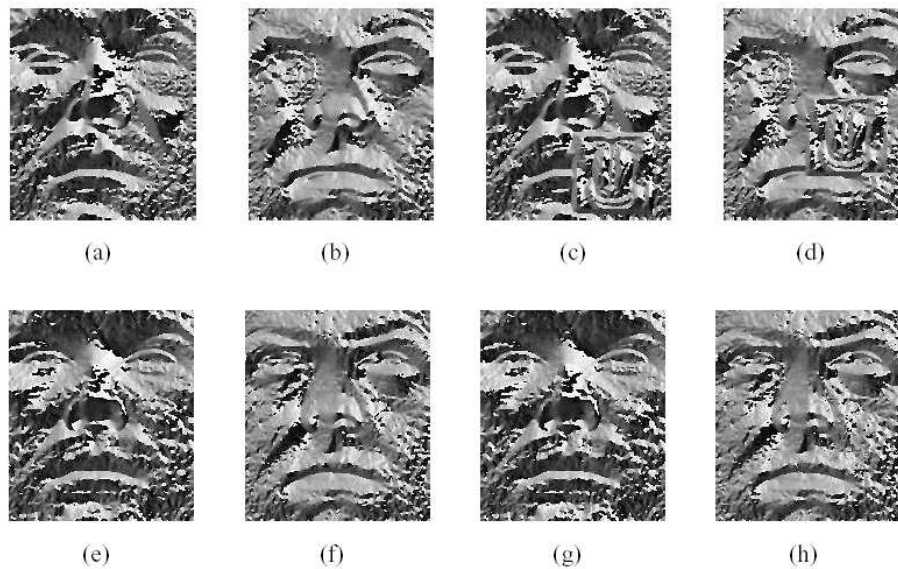


Fig. 5. PCA-based reconstruction of gradient orientations. (a)-(b) Original orientations used in version 1 of our experiment. (c)-(d) Corrupted orientations used in version 2 of our experiment. (e)-(f) Reconstruction of (a)-(b) with 5 principal components. (g)-(h) Reconstruction of (c)-(d) with 5 principal components.

REFERENCES

- [1] N.A. Campbell, *Robust procedures in multivariate analysis I: Robust Covariance estimation*, Applied Statistics, 29 (1980), pp. 231–237.

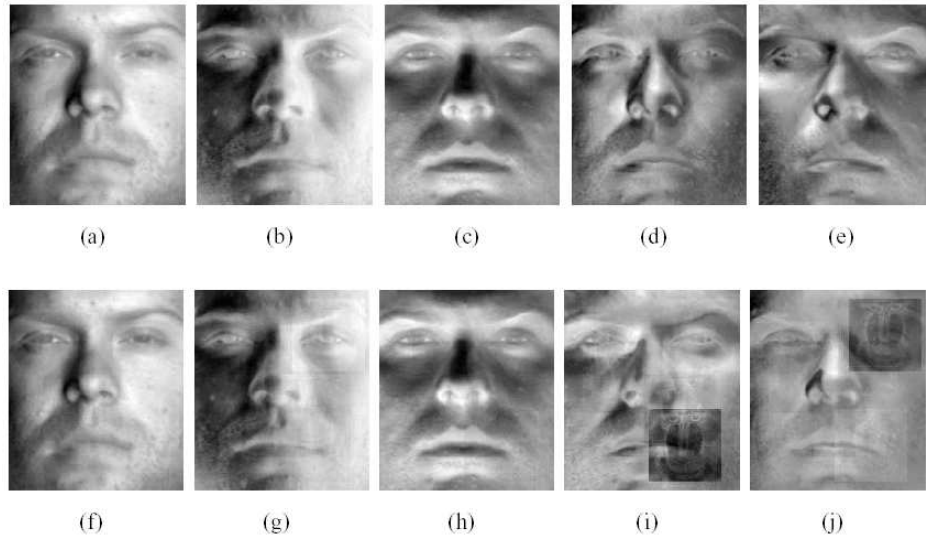


Fig. 6. The 5 principal components of pixel intensities for (a)-(e) version 1 and (f)-(j) version 2 of our experiment.

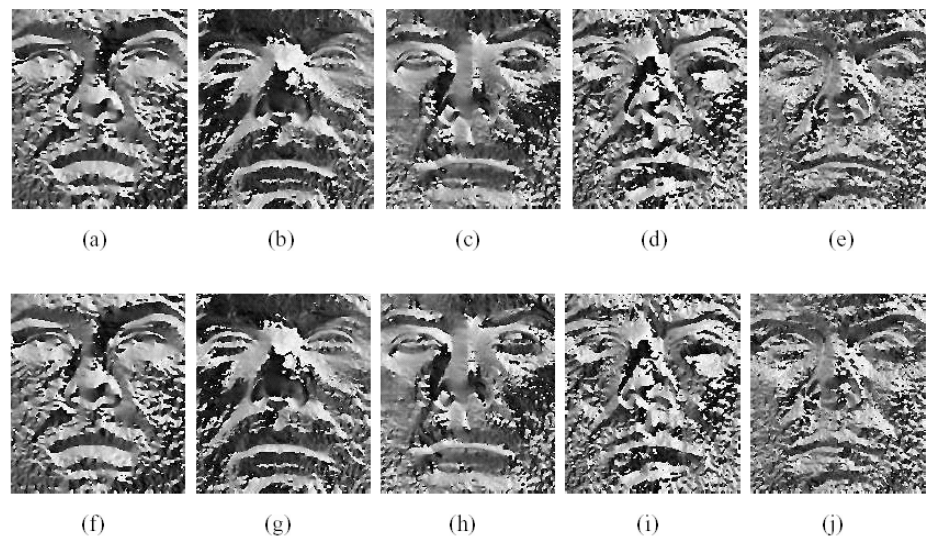


Fig. 7. The 5 principal components of gradient orientations for (a)-(e) version 1 and (f)-(j) version 2 of our experiment.

- [2] C. Croux and G. Haesbroeck, *Principal component analysis based on robust estimators of the covariance or correlation matrix: influence functions and efficiencies*, *Biometrika*, 87 (2000), pp. 603.
- [3] Q. Ke and T. Kanade, *Robust $L1$ norm factorization in the presence of outliers and missing data by alternative convex programming*, in *IEEE Computer Society Conference on Computer Vision and Pattern Recognition, CVPR (2005)*.
- [4] N. Kwak, *Principal component analysis based on $L1$ -norm maximization*, *IEEE transactions on pattern analysis and machine intelligence*, 30 (2008), pp. 1672–1680.
- [5] F.D.L. Torre and M.J. Black, *A framework for robust subspace learning*, *International Journal of Computer Vision*, 54

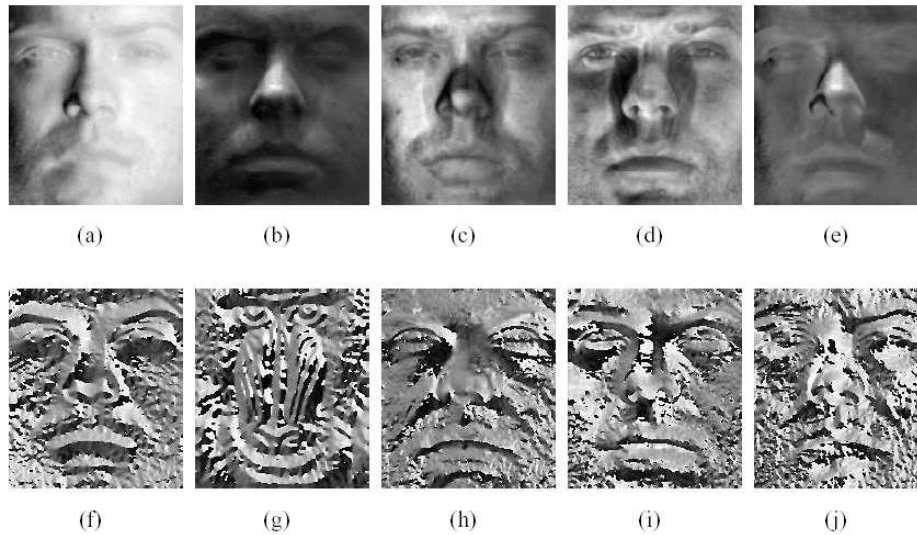


Fig. 8. (a)-(e) The 5 principal components of pixel intensities for version 3 of our experiment and (f)-(j) The 5 principal components of gradient orientations for the same experiment.

(2003), pp. 117–142.

- [6] V. Chandrasekaran, S. Sanghavi, P.A. Parrilo and A.S. Willsky, *Rank-sparsity incoherence for matrix decomposition*, preprint, (2009).
- [7] E.J. Candes, X. Li, Y. Ma, and J. Wright, *Robust principal component analysis?*, Arxiv preprint arXiv:0912.3599, (2009).
- [8] G. Tzimiropoulos, V. Argyriou, S. Zafeiriou, and T. Stathaki, *Robust FFT-Based Scale-Invariant Image Registration with Image Gradients*, IEEE Transactions on Pattern Analysis and Machine Intelligence, accepted for publication (2010).
- [9] M. Turk and A.P. Pentland, *Eigenfaces for recognition*, Journal of Cognitive Neuroscience, 3 (1991), pp. 71–86.
- [10] A.J. Fitch, A. Kadyrov, W.J. Christmas, and J. Kittler, *Orientation correlation*, in British Machine Vision Conference, 1 (2002), pp. 133–142.
- [11] H.P. Frey, P. Konig, and W. Einhauser, *The Role of First and Second-Order Stimulus Features for Human Overt Attention*, Perception and Psychophysics, 69 (2007), pp. 153–161.
- [12] A. Papoulis and S.U. Pillai, *Probability, random variables, and stochastic processes*, McGraw-Hill New York (2004).
- [13] M. Kirby and L. Sirovich, *Application of the karhunen-loeve procedure for the characterization of human faces*, IEEE Transactions Pattern Analysis and Machine Intelligence, 12 (1990), pp. 103–108.
- [14] A.S. Georghiades, P.N. Belhumeur and D.J. Kriegman, *From few to many: Illumination cone models for face recognition under variable lighting and pose*, IEEE Transactions on Pattern Analysis and Machine Intelligence, 23 (2001), pp. 643–660.
- [15] A.M. Martinez and R. Benavente, *The AR face database*, Tech. Rep., CVC Technical report (1998).